Energy Transfer, Electron Transfer, and Addition Reactions of Triplet State of 1,3-Dihydroimidazole-2-thiones Investigated by Laser Flash Photolysis

Maksudul M. Alam and Osamu Ito*

Institute for Chemical Reaction Science, Tohoku University, Katahira, Aoba-ku, Sendai 980-8577

(Received June 9, 1998)

The transient absorption bands observed at ca. 400 and 550 nm for 1,3-dihydro-2*H*-imidazole-2-thione (IT), 1,3-dihydro-1-methyl-2*H*-imidazole-2-thione (MIT), and 1,3-dihydro-2*H*-benzimidazole-2-thione (BIT) have been assigned to their triplet states (^{3}IT* 's) by the quenching and sensitizing experiments using laser flash photolysis technique. Short intrinsic triplet lifetimes and relatively high triplet energies have been evaluated as characteristics of ^{3}IT* 's. For electron acceptors, photoinduced electron-transfer reaction occurs via ^{3}IT* 's in the diffusion controlled limit. The nucleophilic character of ^{3}IT* 's was confirmed by changing the substituents of alkenes on the addition reactions. MO calculations indicate that the lowest electronic configurations of both ^{3}IT* and ^{3}MIT* have $^3(n,\pi^*)$ character, while ^{3}BIT* has $^3(\pi,\pi^*)$ character. The addition reactivity of ^{3}BIT* is slightly higher than those of ^{3}IT* and ^{3}MIT*, which is opposite to the general tendency.

Photochemical properties of the excited state of aliphatic thiones and aromatic thiones have been studied and they were compared with the results of ketone photochemistry.[1—8] The photochemistry of the aromatic thiones possessing nitrogen atoms is highly important from the chemical[9,10] and the biological[11,12] viewpoints. Chemically, various interesting photochemical reactions are known for pyridinethiones.[9,10] In our previous studies, the photochemical properties of pyridinethiones (PyT) and 1,7-dihydro-6*H*-purine-6-thione (PuT) have been revealed by means of laser flash photolysis.[13] The photochemical properties such as energy transfer, electron transfer, hydrogen abstraction and addition reaction were attributed to the triplet states of the thione-forms.[13] One of the characteristics is their high electron-transfer abilities; thione triplet states act as both electron donor and electron acceptor, depending on the additives.[13] From the addition reaction to substituted alkenes and the H-atom abstraction reaction, the electrophilic nature of the triplet states of PyT and PuT has been revealed.[13]

In the present study, we employed three dihydroimidazolethione derivatives (IT's), which mainly exist in the thione form.[14,15] Since the IT moiety possesses two N atoms in the vicinal of >C=S, as shown in Scheme 1, different properties and reactivities would be anticipated in their triplet state from those of PyT and PuT,[13] which have one vicinal N atom.

In addition, since the compounds possessing the IT moiety are well known as corrosion inhibitors under high radiation,[16,17] it is important to investigate the reactive intermediate species produced from IT's by photochemical methods such as laser-flash photolysis. In order to confirm the experimentally observed results, we also performed some molecular orbital calculations.

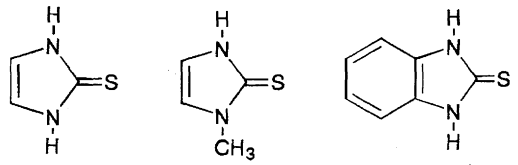

IT: 1,3-Dihydro-2*H*-imidazole-2-thione

MIT: 1,3-Dihydro-1-methyl-2*H*-imidazole-2-thione

BIT: 1,3-Dihydro-2*H*-benzimidazole-2-thione

Scheme 1. Structures of dihydroimidazolethione compounds.

Experimental

Materials and Steady-State Measurements. 1,3-Dihydro-2*H*-imidazole-2-thione (IT), 1,3-dihydro-1-methyl-2*H*-imidazole-2-thione (MIT), and 1,3-dihydro-2*H*-benzimidazole-2-thione (BIT) were obtained from Aldrich Chemical Co. in a purity of > 99%. Commercially available dinitrobenzenes (DNB), triplet quenchers and alkenes (purity > 98%) were used after purification. Solvents used for the transient absorption measurements were of spectroscopic grade. Absorption spectra of the radical ions of IT's were measured by the γ-irradiation in frozen glassy butyl chloride at 77 K.

Transient Absorption Measurements. Nanosecond laser photolysis apparatus was a standard design with fourth harmonic generator (FHG; 266 nm) and third harmonic generator (THG; 355 nm) lights from Nd:YAG laser (Quanta-Ray, 6 ns fwhm).[18] Transient spectra and time profiles in the visible region were followed by a photomultiplier tube (PMT) as a detector for monitoring light from continuous Xe-monitor lamp (150 W). In the visible and near-IR regions (350—1000 nm), an Si-PIN photodiode attached to a

monochromator was employed as a detector to monitor the probe light from a pulsed Xe-flash lamp. Deaerated and O_2-saturated solutions were obtained by Ar and O_2 gas bubbling, respectively, in a rectangular quartz cell with a 10 mm optical path. All measurements were carried out at 23 °C.

MO Calculations. The MO calculations were performed with Modified Neglect of Differential Overlap (MNDO) method using a general Molecular Orbital Package (MOPAC) presented by the Japan Program Exchange Association.[19]

Results and Discussion

Steady-State Absorption Spectra. Figure 1 shows the absorption spectra of IT and MIT (0.1×10^{-3} mol dm^{-3}) in THF. The sharp absorption band of both at 269 nm (ε = 15800 and 16000 mol^{-1} dm^3 cm^{-1} for IT and MIT, respectively) was attributed to $^1(\pi$–$\pi^*)$ transition,[1,3,6,8] while the absorption tail in the region of 300—325 nm (ε = 200—270 mol^{-1} dm^3 cm^{-1}) may be assigned to $^1(n$–$\pi^*)$ transition of >C=S chromophore.[1,3,6,8]

In the case of BIT, the absorption peak appears at 315 nm (ε = 17000 mol^{-1} dm^3 cm^{-1}), as shown in Fig. 1, and is assignable to $^1(\pi$–$\pi^*)$ transition.[1,3,6,8] The absorption tail of $^1(n$–$\pi^*)$ transition, which is assumed to be very weak and hidden by the intense band at 315 nm, was not observed even at higher concentrations.

In all cases, the spectral shape of the dilute solution (0.05×10^{-3} mol dm^{-3}) is the same as that of the concentrated solution (up to 1.0×10^{-3} mol dm^{-3}). The absorption intensities increase proportionally with concentration, obeying the Beer–Lambert law, indicating that aggregation of IT's may not be appreciable in the concentration range of (0.05—$1.0)\times10^{-3}$ mol dm^{-3}.

Transient Absorption Spectra. Transient absorption spectra observed by the laser photolysis of IT (0.1×10^{-3} mol dm^{-3}) with 266 nm light in Ar-saturated THF exhibit a main absorption peak at 540 nm with a weak one at 380 nm, as shown in Fig. 2. The absorption intensities of both bands, which decrease within about 5 μs in THF, were effectively quenched by O_2 (inset in Fig. 2) and other triplet quenchers, suggesting that the 540 and 380 nm absorptions are due to the triplet–triplet (T–T) transition of ^{3}IT*.

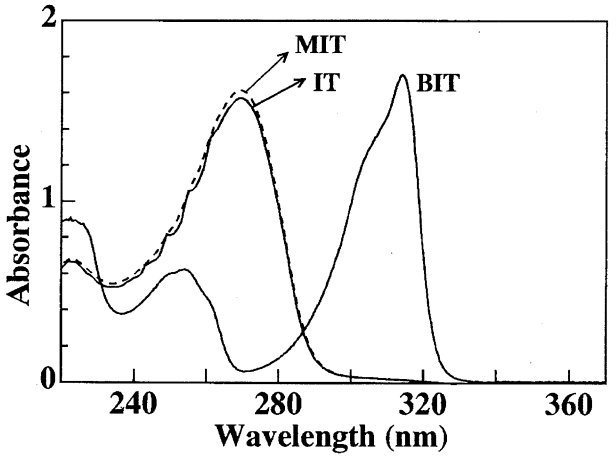

Fig. 1. Steady UV/visible absorption spectra of IT's (0.1×10^{-3} mol dm^{-3}) in THF with 1.0 cm of optical path.

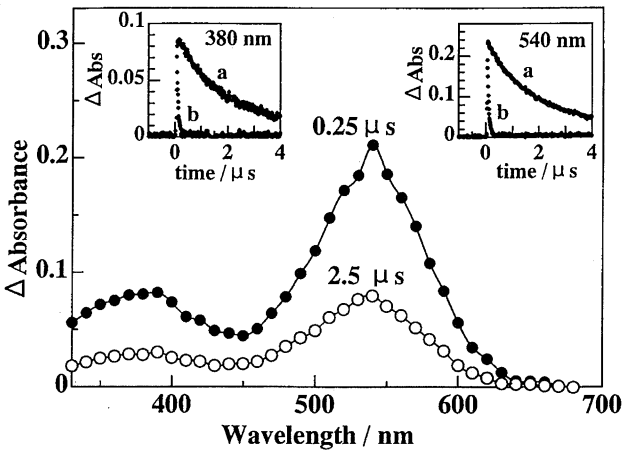

Fig. 2. Transient absorption spectra observed after laser photolysis of IT (0.1×10^{-3} mol dm^{-3}) with 266 nm light in Ar-saturated THF (PMT as detector). Insert: Time-profiles of absorption bands; (a) in Ar-saturated and (b) in aerated solutions.

Similar transient absorption spectra were observed by the laser photolysis of MIT and BIT with 266 nm light in Ar-saturated THF. ^{3}MIT* shows absorptions at 540 and 380 nm. For ^{3}BIT*, appearance of T–T absorption bands in longer wavelength region (at 570 and 390 nm) may be due to the extension of π-conjugation in BIT.

As self-quenching (Eq. 2) is one of the characteristics of the triplet states of thiones,[3,8,13] the triplet-decay lifetimes (τ_T) of ^{3}IT* 's were measured as a function of ground-state concentration of IT's with low laser powers (2.0—5.0 mJ pulse^{-1}). For the decay of ^{3}IT* 's, the first-order rate constant ($k_T = 1/\tau_T$) increases with [IT's]. The self-quenching rate constant (k_{sq}) and the intrinsic triplet lifetime (τ_T°) can be evaluated from Eq. 3,[2,13] as summarized in Table 1.

$$^3\mathrm{IT}^* \xrightarrow[\tau_T^\circ]{k_T} \mathrm{IT} \quad (1)$$

$$^3\mathrm{IT}^* + \mathrm{IT} \xrightarrow{k_{sq}} \mathrm{IT} + \mathrm{IT} \quad (2)$$

$$1/\tau_T = 1/\tau_T^\circ + k_{sq}[\mathrm{IT}] \quad (3)$$

The τ_T° values of these thiones are smaller than those of

Table 1. Triplet Absorption Maxima (λ_{max}^T), Molar Extinction Coefficient (ε), Intrinsic Triplet Lifetime (τ_T°), and Self-quenching Rate Constants (k_{sq}) of ^{3}IT*, ^{3}MIT*, and ^{3}BIT* in THF at 23 °C

^{3}IT* 's	λ_{max}^{T} a) (ε_T)b)	τ_T°c)	k_{sq}c)
	(nm) (mol^{-1} dm^3 cm^{-1})	(μs)	(mol^{-1} dm^3 s^{-1})
^{3}IT*	380, 540 (6550)	2.0	4.1×10^8
^{3}MIT*	380, 540 (6440)	2.1	4.3×10^8
^{3}BIT*	390, 570 (6100)	1.5	3.6×10^8

a) Each λ_{max} value contains estimation error of ±2 nm. b) ε_T was estimated by energy transfer method in benzene and each ε_T value contains estimation error of ±5%. c) Intrinsic triplet lifetime (τ_T°) was estimated by the extrapolation to infinite dilution in the plots of k_T ($1/\tau_T$) vs. [IT]; k_{sq} was evaluated from the slope.

aromatic carbonyl compounds. The short τ_T°, which is one of the characteristics of the triplet states of thiones, may be caused by T_1–S_0 deactivation process due to the spin-orbit coupling of the S atom.[6,8,13]

On addition of other triplet quenchers,[13,21,22] the bimolecular quenching rate constants (k_q in Eq. 4) were evaluated from the pseudo first-order plots. The k_q values thus obtained are summarized in Table 2. In the present study, formation of singlet O_2 was confirmed by consumption of 1,3-diphenylisobenzofuran.[13,20] Although the k_q values for 1,3-cyclohexadiene (1,3-CHD; E_{T_1} = 52.4 kcal mol^{-1})[13,22] are still close to the diffusion controlled limit (k_{diff}), the k_q values for ^{3}IT* and ^{3}MIT* with 2-methyl-1,3-butadiene (isoprene; E_{T_1} = 60.1 kcal mol^{-1}),[13,22] are about 1/100—1/200 of k_{diff}. Since the k_q values depend on the difference between the T_1-energies, they are all attributed to the triplet energy-transfer rate constants. Therefore, the E_{T_1} values are calculated to be 57.3 kcal mol^{-1} for ^{3}IT* and 57.0 kcal mol^{-1} for ^{3}MIT* using the Sandros equation.[23] For ^{3}BIT*, the k_q value with isoprene is still close to k_{diff}. Thus, the E_{T_1} value of ^{3}BIT* was evaluated to be 61.3 kcal mol^{-1}.

$$^3\text{IT}^* + \text{quencher} \xrightarrow{k_q} \text{IT} + {}^3(\text{quencher})^* \quad (4)$$

On steady-light photolysis in the presence of isoprene, no change of absorption intensity of IT's was observed, which confirmed that the bimolecular experimental rate constants are due to energy transfer from ^{3}IT* 's to isoprene, but not due to the addition reaction.

Sensitized Formation of ^{3}IT* 's. Using 355 nm light which excites only the thioxanthone (TXN), the sensitized formation of ^{3}IT* 's was observed by energy transfer from ^{3}TXN* (E_{T_1} = 65.5 kcal mol^{-1})[22] to IT's (Fig. 3) in Ar-saturated benzene (Eq. 5).

$$\text{TXN} \xrightarrow[(355\ \text{nm})]{h\nu} {}^3\text{TXN}^* \xrightarrow[k_{ent}]{\text{IT}} {}^3\text{IT}^* + \text{TXN} \quad (5)$$

The decay rate of the absorption band of ^{3}TXN* at 660 nm,[24] which has a long lifetime (τ_T = 95 μs in benzene)[24] in the absence of IT, was increased by the addition of IT, as shown in the inset in Fig. 3. ^{3}TXN* has also weak absorption in the region of 500—600 nm.[24] However, the absorption band at 540 nm does not seem to decay due to the overlap of the rise of absorption band of ^{3}IT* at 540 nm (inset in Fig. 3). From the decay time-profiles of the absorption band of ^{3}TXN* at 660 nm, the rate constants (k_{ent}) for energy transfer from ^{3}TXN* to IT, MIT, and BIT in benzene were evaluated to be 7.1×10^9, 6.9×10^9, and 5.5×10^9 mol^{-1} dm^3 s^{-1}, respectively.

Table 2. Quenching Rate Constants (k_q) for Reactions of ^{3}IT*, ^{3}MIT*, and ^{3}BIT* with Triplet Quenchers at 23 °C in THF

Quenchers	E_{T_1}	k_q[a]/mol^{-1} dm^3 s^{-1}		
	kcal mol^{-1}	^{3}IT*	^{3}MIT*	^{3}BIT*
O_2	22.5[c]	3.5×10^9	3.9×10^9	3.3×10^9
Ferrocene	42.9[d]	2.3×10^9	2.4×10^9	2.1×10^9
1,3-CHD[b]	52.4[c]	2.1×10^9	1.9×10^9	1.7×10^9
Isoprene	60.1[c]	8.9×10^7	7.6×10^7	1.4×10^9

a) Estimation error is ±5%. b) CHD: cyclohexadiene. c) Ref. 22. d) Ref. 21.

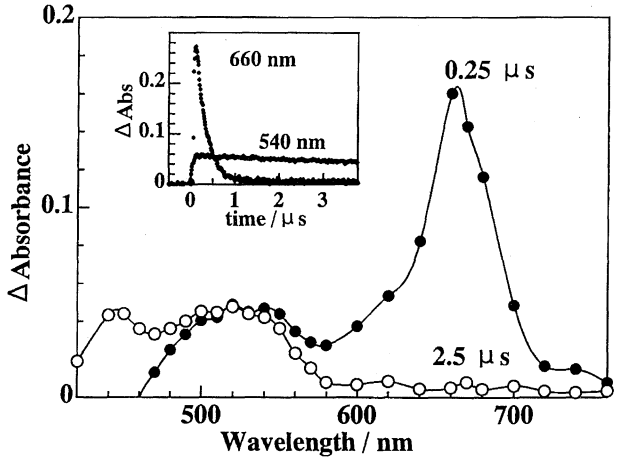

Fig. 3. Transient absorption spectra observed after laser photolysis of thioxanthone (0.1×10^{-3} mol dm^{-3}) in the presence of IT (0.4×10^{-3} mol dm^{-3}) with 355 nm light in Ar-saturated benzene (PMT as detector). Insert: Time-profiles of absorption bands.

The molar extinction coefficients (ε_{IT}) of ^{3}IT* 's were estimated from the reported ε_{TXN} (= 30000 mol^{-1} dm^3 cm^{-1} at 660 nm)[24] value for ^{3}TXN* using Eq. 6, assuming the energy transfer efficiency is one. This assumption may be satisfied because of a large triplet-state energy difference (ΔE_{T_1} = 6—9 kcal mol^{-1}) between TXN and IT's.

$$\varepsilon_{IT} = \Delta A_{IT}(\varepsilon_{TXN}/\Delta A_{TXN}) \quad (6)$$

Here ΔA's are the absorbance of triplet maxima. These ε_{IT} values of ^{3}IT* 's in benzene are determined to be 6000—7000 mol^{-1} dm^3 cm^{-1} as listed in Table 1.

Photoinduced Electron Transfer. The transient absorption spectra observed by laser photolysis (with 266 nm light) of IT (0.1×10^{-3} mol dm^{-3}) in the presence of *p*-dinitrobenzene (*p*-DNB; 0.4×10^{-3} mol dm^{-3}) in Ar-saturated acetonitrile are shown in Fig. 4. The sharp absorption peak of ^{3}IT* at 540 nm decays along with the appearance of new absorption bands at 360, 840, and 910 nm, which are assigned to the radical anion of *p*-DNB (*p*-DNB$^{\bullet-}$).[13,25,26] The decay curve of ^{3}IT* at 540 nm and the rise curves of *p*-DNB$^{\bullet-}$ at 360 and 910 nm are shown in the inset of Fig. 4.

The 540 nm band of ^{3}IT* did not seem to decay completely, because of the overlap of the rise of the absorption band of IT$^{\bullet+}$. The formation of IT$^{\bullet+}$ at 530 nm was confirmed, since a similar absorption band was observed by γ-irradiation of IT in butyl chloride at 77 K. Similarly, the absorption bands for MIT$^{\bullet+}$ at 530 nm and for BIT$^{\bullet+}$ at 560 nm were observed.

The rate constants (k_q) obtained from the decay profiles of ^{3}IT* are in good agreement with those obtained from the rise profiles of *p*-DNB$^{\bullet-}$ in acetonitrile. Thus, it is evident that the quenching of ^{3}IT* by *p*-DNB producing *p*-DNB$^{\bullet-}$

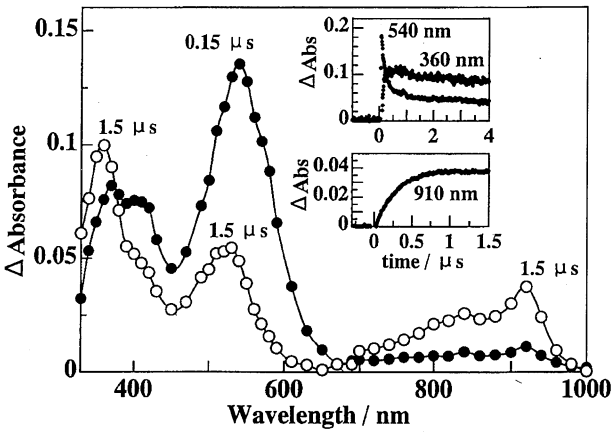

Fig. 4. Transient absorption spectra in the visible/near-IR region obtained by 266 nm laser photolysis of IT (0.1×10^{-3} mol dm^{-3}) in the presence of *p*-DNB (0.4×10^{-3} mol dm^{-3}) in Ar-saturated acetonitrile (Si-PIN as detector). Insert: Time-profiles of absorption bands.

in acetonitrile can be attributed to the electron-transfer reaction from ^{3}IT* to *p*-DNB (Eq. 7).[13,25] Similarly, the electron-transfer reactions were observed for MIT and BIT with *p*-DNB and also with *m*- and *o*-DNB. The sharp absorption bands of DNB$^{\bullet-}$ and IT$^{\bullet+}$ may be assigned to the free radical ions, but not to geminate ion pair. Thus, the quantum yields Φ_{et} for the formation of DNB$^{\bullet-}$ via ^{3}IT* 's were evaluated from the ratio $[DNB^{\bullet-}]/[^3IT^*] = (A_{ar}/\varepsilon_{ar})/(A_T/\varepsilon_T)$ upon substituting the observed absorption intensities (A_{ar} refers to maximum absorbance of DNB$^{\bullet-}$ and A_T to initial absorbance of ^{3}IT*) and extinction coefficients (ε_T refers to that of ^{3}IT* 's and ε_{ar} to that of DNB$^{\bullet-}$).[13,25,26] They are listed in Table 3. The Φ_{et} values are less than unity in acetonitrile, which indicates that some other deactivation processes (k_d in Eq. 7) take place competitively with the electron-transfer reaction. Thus, the electron-transfer rate constants (k_{fet}) via ^{3}IT* 's were calculated by the relation $k_{fet} = \Phi_{et}k_{obsd}$[27] as listed in Table 3.

Table 3. Rate Constants for Forward Electron-transfer (k_{fet}) and Back Electron Transfer (k_{bet}) and Electron-transfer Quantum Yield (Φ_{et}) of ^{3}IT* 's with DNB in Acetonitrile at 23 °C

Systems	k_{obsd}[a]	Φ_{et}[b]	k_{fet}[c]	k_{bet}[d]
	mol^{-1} dm^3 s^{-1}		mol^{-1} dm^3 s^{-1}	mol^{-1} dm^3 s^{-1}
^{3}IT*/*p*-DNB	7.0×10^9	0.24	1.7×10^9	1.8×10^{10}
^{3}MIT*/*p*-DNB	7.1×10^9	0.26	1.8×10^9	1.6×10^{10}
^{3}BIT*/*p*-DNB	6.1×10^9	0.21	1.3×10^9	1.4×10^{10}
^{3}BIT*/*m*-DNB	4.6×10^9	0.18	8.3×10^8	1.2×10^{10}
^{3}BIT*/*o*-DNB	4.4×10^9	0.20	8.8×10^8	1.3×10^{10}

a) Estimation error is ±5% and obtained from the decay of ^{3}IT* 's by DNB and also from the rise of DNB$^{\bullet-}$ in acetonitrile. b) $\Phi_{et} = [DNB^{\bullet-}]/[^3IT^*$'s] was calculated using the observed absorbance, ε_T of ^{3}IT* 's, and the reported ε_{ra} values of DNB$^{\bullet-}$.[13,25,26] c) $k_{fet} = \Phi_{et}k_{obsd}$.[27] d) Estimation error is ±5% and obtained by using the reported ε_{ra} values of DNB$^{\bullet-}$ in acetonitrile.

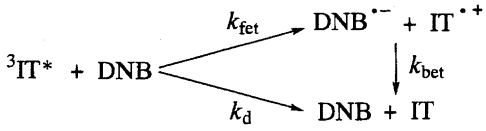

(7)

The observed values of k_{fet} for electron transfer from ^{3}BIT* to *p*-DNB, *m*-DNB, and *o*-DNB (Table 3) follow the same trend as the reported reduction potentials $E_{(A/A^-)}$ = −0.69 eV for *p*-DNB,[28] −0.90 eV for *m*-DNB,[28] and −0.81 eV for *o*-DNB,[28] in acetonitrile.

When the time profiles were observed on long time scales, the intensities of the absorption peaks of the radical ions (IT$^{\bullet+}$ and *p*-DNB$^{\bullet-}$) decay slowly after reaching maxima in acetonitrile. These decays obeying second-order kinetics as shown in Fig. 5 can be attributed to the back electron-transfer reactions (Eq. 7).[13,25]

From the slopes of the second-order plots (inset in Fig. 5), the ratio of the rate constant (k_{bet}) of back electron-transfer to the molar extinction coefficient of radical ions (ε_r) can be obtained. On substituting the reported values of ε_{ra},[13,25] one can evaluate the k_{bet} values for DNB$^{\bullet-}$ in acetonitrile (Table 3). Compared with the reported molar extinction coefficient (ε = 5900 mol^{-1} dm^3 cm^{-1} in acetonitrile) of *p*-DNB$^{\bullet-}$ at 910 nm,[13,25] the extinction coefficients (ε_{rc}) of the radical cations of IT's (IT$^{\bullet+}$'s) were estimated to be 2700, 2650, and 2050 mol^{-1} dm^3 cm^{-1} for IT$^{\bullet+}$ (at 530 nm), MIT$^{\bullet+}$ (at 530 nm), and BIT$^{\bullet+}$ (at 560 nm), respectively, in acetonitrile.

Addition Reaction to Alkenes. The decay rates of the absorption bands of ^{3}IT* 's increase with increasing the concentration of alkene; cycloaddition reaction is most probable for ^{3}IT* 's, similar to other aromatic thiones.[4,13,29] Stepwise cycloaddition can be considered as a main route for the addition reaction of ^{3}IT* 's to alkenes as in Eq. 8.[4,13,29] The rate constants (k_{ad}) for the addition reaction of ^{3}IT* 's with several alkenes are summarized in Table 4 with the Alfrey–Price's *e*-values,[13,30]) which are a measure of the electron density of C=C. The k_{ad} values for the addition reaction of

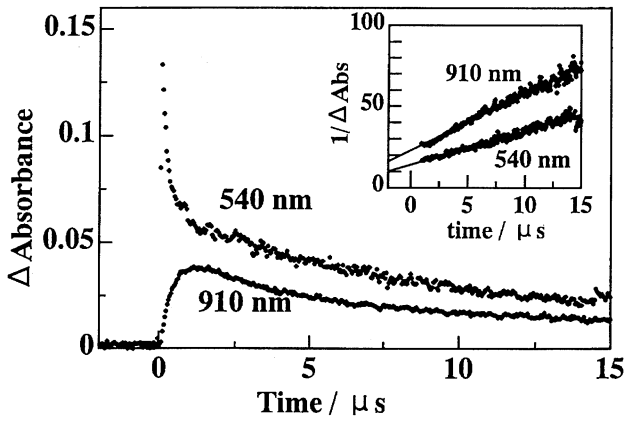

Fig. 5. Absorption-time profiles for the decay of IT$^{\bullet+}$ (at 540 nm) and *p*-DNB$^{\bullet-}$ (at 910 nm) obtained by 266 nm laser photolysis of IT (0.1×10^{-3} mol dm^{-3}) with *p*-DNB (0.4×10^{-3} mol dm^{-3}) in Ar-saturated acetonitrile. Insert: Second-order plots.

Table 4. Rate Constants (k_{ad}) for Addition Reaction of ^{3}IT*'s in THF and Alfrey–Price's *e*-values of Alkenes

Alkenes	(abb)	k_{ad}[a]/mol^{-1} dm^3 s^{-1}			
		^{3}IT*	^{3}MIT*	^{3}BIT*	*e*-value[b]
CH_2=C(CH_3)CO_2CH_3	(MMA)	7.8×10^7	5.2×10^7	1.9×10^8	0.40
CH_2=C(CH_3)CN	(MAN)	1.9×10^8	1.6×10^8	3.9×10^8	0.61
CH_2=CHCN	(AN)	4.2×10^8	4.7×10^8	6.7×10^8	1.20

a) Estimation error is ±5%. b) *e*-values of alkenes are cited from Refs. 13 and 30.

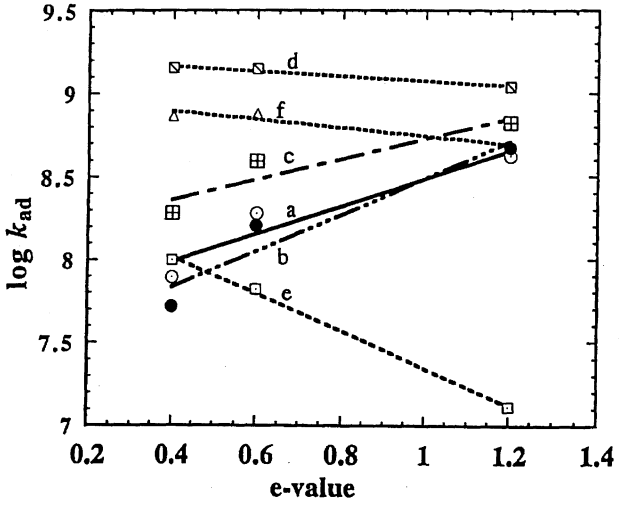

Fig. 6. Plots of log k_{ad} for ^{3}IT* 's against Alfrey–Price's *e*-values of different alkenes in Ar-saturated THF; (a) ^{3}IT*, (b) ^{3}MIT*, (c) ^{3}BIT*, (d) ^{3}4PyT*, (e) ^{3}2PyT*, and (f) ^{3}PuT*.

^{3}IT* 's to various alkenes are plotted against Alfrey–Price's *e*-values, as shown in Fig. 6.

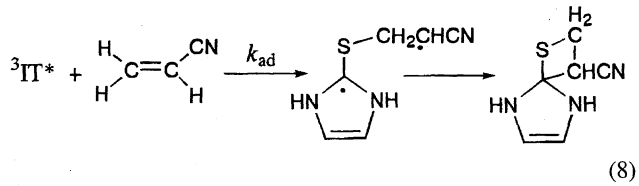

(8)

The slope of the plot is a measure of the polar character of the attacking ^{3}IT* 's. Positive slopes suggest the nucleophilicity of ^{3}IT* 's with respect to C=C;[13,29,30] which is in accordance with the reported findings for IT's by Arbelot et al.[31] and Gentric et al.[32] The nucleophilic nature of ^{3}IT* 's indicates that a partial charge-transfer character from ^{3}IT* 's to alkenes occurs in the transition state during the addition reaction.[13,29,30]

The magnitudes of the positive slope for both ^{3}IT* and ^{3}MIT* are greater than that of ^{3}BIT* (Fig. 6), which suggests that the nucleophilic nature of ^{3}BIT* is less than those of ^{3}IT* and ^{3}MIT* due to the delocalization of the π-electron over ^{3}BIT*. Furthermore, we observed that the addition reactivity of ^{3}BIT* to alkenes is higher than those of ^{3}IT* and ^{3}MIT* (Table 4). Thus, this finding can be explained as follows: The higher the nucleophilicity, the lower is the addition reactivity to alkenes, in accord with the reactivity-selectivity principle.[33]

MO Calculations. Electron densities of ^{3}IT* 's were calculated by the unrestricted open-shell Hartree–Fock

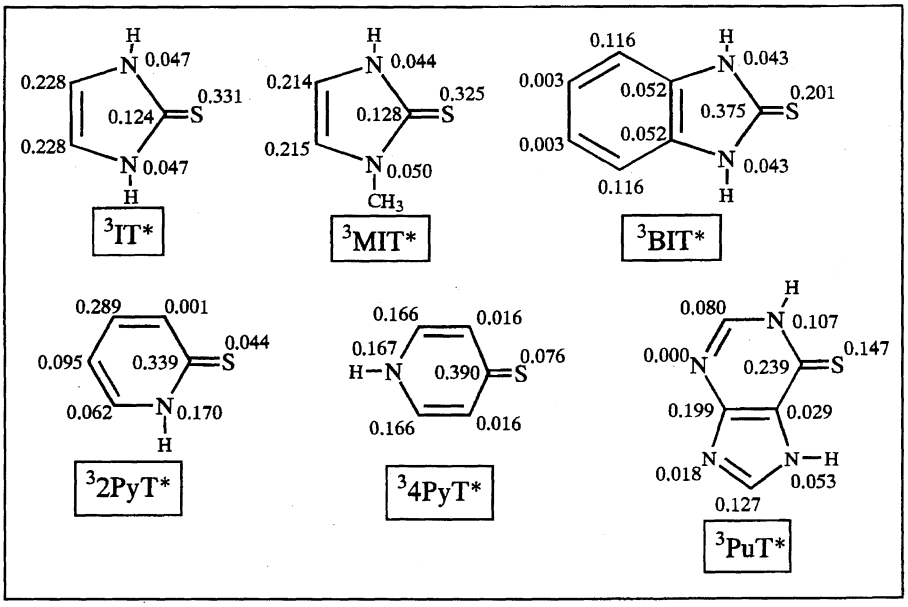

Fig. 7. Unpaired π-electron density of upper SOMO level of triplet state of thiones calculated by MOPAC.

(ROHF) method on the geometries optimized at the MNDO/CI level using the MOPAC program package.[13,19] In two singly occupied levels (SOMO) of each triplet excited state, the unpaired π-electron density on the S-atom may be a measure of the nucleophilicity. The π-electron densities on the S-atom of the upper SOMO of both ^{3}IT* and ^{3}MIT* are higher than that of ^{3}BIT*, as shown in Fig. 7, which suggests that the nucleophilic nature of ^{3}BIT* is less than those of ^{3}IT* and ^{3}MIT*. This is in good agreement with the experimentally observed nucleophilicity for the addition reaction of ^{3}IT* 's to alkenes (Table 4). On the other hand, the electrophilic nature of the triplet states of pyridinethiones (^{3}PyT*) and 1,7-dihydro-6*H*-purine-6-thione (^{3}PuT*) (Figs. 6 and 7) was found in our previous study.[13] This was confirmed by the quite low π-electron densities on the S-atom of the upper SOMO of ^{3}PyT* and ^{3}PuT* (Fig. 7).

In the cases of ^{3}IT* and ^{3}MIT*, the electron density of C=S at lower SOMO level locates on p_x or p_y plane (n-character), while the upper SOMO level locates on p_z-plane (π-character). This indicates the $^3(n,\pi^*)$-configuration of the lowest triplet level for both ^{3}IT* and ^{3}MIT*. For ^{3}BIT*, the electron density of C=S is at the p_z-plane (π-character) in both the lower and upper SOMO levels, indicating that the lowest electronic level has $^3(\pi,\pi^*)$ character.

Concluding Remarks

Most of the properties of ^{3}IT* 's are common with those of ^{3}PyT* and ^{3}PuT*. High electron-donor ability has also been observed for ^{3}IT* 's with DNB in polar solvents, while electron-acceptor ability of ^{3}IT* 's is lower than that of ^{3}PyT* and ^{3}PuT*. The addition reactivities of ^{3}IT* 's to the double bonds of alkenes were also high; however, the experimental data indicate the nucleophilic character of ^{3}IT* 's, while ^{3}PyT* and ^{3}PuT* have the opposite character, as was supported by MO calculations. The lowest electronic states of both ^{3}IT* and ^{3}MIT* have $^3(n,\pi^*)$ character, whereas ^{3}BIT* has $^3(\pi,\pi^*)$ character. In the case of the triplet state of >C=O, in general, the reactivity of $^3(\pi,\pi^*)$ is far lower than that of $^3(n,\pi^*)$. However, such a difference was not found for ^{3}IT* 's.

The present work was partly supported by a Grant-in-Aid on Priority-Area-Research on "Carbon Alloys" (No. 10137203) from the Ministry of Education, Science, Sports and Culture. The authors would like to thank to Mr. S. Furukawa of ^{60}Co-center in Tohoku University for his assistance with γ-irradiation.

References

1) a) J. Wirz, *J. Chem. Soc., Perkin Trans. 2*, **1973**, 1307; b) P. de Mayo, *Acc. Chem. Res.*, **9**, 52 (1976).

2) C. V. Kumar, L. Qin, and P. K. Das, *J. Chem. Soc., Faraday Trans. 2*, **80**, 783 (1984).

3) A. Maciejewski, D. R. Demmer, D. R. James, A. Safarzadeh-Amiri, R. E. Verrall, and R. P. Steer, *J. Am. Chem. Soc.*, **107**, 2831 (1985).

4) J. Kamphuis, H. J. T. Bos, R. J. Visser, B. H. Huizer, and C. A. G. O. Varma, *J. Chem. Soc., Perkin Trans. 2*, **1986**, 1867.

5) K. Bhattachayya, V. Ramamurthy, and P. K. Das, *J. Phys. Chem.*, **91**, 5626 (1987).

6) a) A. Maciejewski, M. Syzmanski, and R. P. Steer, *J. Phys. Chem.*, **92**, 6939 (1988); b) V. Ramamurthy and R. P. Steer, *Acc. Chem. Rev.*, **21**, 380 (1988).

7) R. Minto, A. Samanta, and P. K. Das, *Can. J. Chem.*, **67**, 967 (1989).

8) A. Maciejewski and R. P. Steer, *Chem. Rev.*, **93**, 67 (1993).

9) a) D. H. R. Barton, D. Crich, and W. B. Motherwell, *Tetrahedron*, **41**, 3901 (1985); b) D. H. R. Barton and S. Z. Zard, *Pure Appl. Chem.*, **58**, 675 (1986).

10) a) M. Newcomb and U. Park, *J. Am. Chem. Soc.*, **108**, 4132 (1986); b) M. Newcomb and J. Kaplan, *Tetrahedron Lett.*, **28**, 1615 (1987); b) J. Boivin, E. Crepon, and S. Z. Zard, *Tetrahedron Lett.*, **31**, 6869 (1990).

11) a) E. Shaw, J. Bernstein, K. Loser, and W. A. Lott, *J. Am. Chem. Soc.*, **72**, 4362 (1950); b) A. Albert, "Selective Toxicity: The Physico-Chemical Basis of Therapy," 7th ed, Chapman and Hall, London (1985).

12) a) G. J. Kontoghiorghes, A. Piga, and A. V. Hoffbrand, *Hematolog. Oncol.*, **4**, 195 (1986); b) W. Adam, J. Cadet, F. Dall'Acqua, D. Ramaiah, and C. R. Saha-Moller, *Angew. Chem.*, **107**, 91 (1995).

13) a) M. M. Alam, M. Fujitsuka, A. Watanabe, and O. Ito, *J. Phys. Chem. A*, **102**, 1338 (1998); b) M. M. Alam, M. Fujitsuka, A. Watanabe, and O. Ito, *J. Chem. Soc., Perkin Trans. 2*, **1998**, 817.

14) a) C. W. N. Cumper and G. D. Pickering, *J. Chem. Soc., Perkin Trans. 2*, **1972**, 2045; b) E. Bojarska-Olejnik, L. Stefaniak, M. Witanowski, B. T. Hamdi, and G. A. Webb, *Magn. Reson. Chem.*, **23**, 166 (1985).

15) E. Bojarska-Olejnik, L. Stefaniak, G. A. Webb, and I. H. Sadler, *Bull. Polish Acad. Sci., Chem.*, **35**, 81 (1987).

16) V. G. Ushakov, G. L. Makorei, V. K. Bagin, and V. R. Koroleva, *Zashch. Met.*, **23**, 430 (1987).

17) G. R. Dey, D. B. Naik, K. Kishore, and P. N. Moorthy, *Res. Chem. Intermed.*, **21**, 47 (1995).

18) a) A. Watanabe and O. Ito, *J. Phys. Chem.*, **98**, 7736 (1994); b) M. M. Alam, A. Watanabe, and O. Ito, *J. Org. Chem.*, **60**, 3440 (1995); c) M. M. Alam, H. Konami, A. Watanabe, and O. Ito, *J. Chem. Soc., Perkin Trans. 2*, **1996**, 263.

19) a) J. J. P. Stewart, *J. Comput. Chem.*, **10**, 209 (1989); b) J. J. P. Stewart, *Quantum Chem., Prog. Exch. Bull.*, **9**, 10 (1989).

20) H. H. Wasserman and R. W. Murray, in "Singlet Oxygen," Academic Press, New York (1979), Chaps. 5, 6, 8, and 9.

21) A. Farmilo and F. Wilkinson, *Chem. Phys. Lett.*, **34**, 575 (1975).

22) S. L. Murov, "Handbook of Photochemistry," Marcel Dekker, New York (1973).

23) K. Sandros, *Acta Chem. Scand.*, **18**, 2355 (1964).

24) a) T. Werner, *J. Phys. Chem.*, **83**, 320 (1979); b) I. Carmichael and G. L. Hug, "Triplet–Triplet Absorption Spectra of Organic Molecules in Condensed Phases," *J. Phys. Chem. Ref. Data*, ed by R. L. David, Jr., Vol. 15 (1), 1986, p. 174.

25) M. Fujitsuka, T. Sato, T. Shimidzu, A. Watanabe, and O. Ito, *J. Phys. Chem. A*, **101**, 1056 (1997).

26) T. Shida, "Electronic Absorption Spectra of Radical Ions," Physical Science Data 34, Elsevier, Amsterdam (1988).

27) a) M. M. Alam, A. Watanabe, and O. Ito, *J. Photochem. Photobiol., A: Chem.*, **104**, 59 (1997); b) M. M. Alam, A. Watanabe, and O. Ito, *Bull. Chem. Soc. Jpn.*, **70**, 1833 (1997).

28) A. H. Maki and D. H. Geske, *J. Am. Chem. Soc.*, **83**, 1852

(1961).
29) N. J. Turro and V. Ramamurthy, *Tetrahedron Lett.*, **28**, 2423 (1976).
30) a) O. Ito, *Res. Chem. Intermed.*, **21(1)**, 69 (1995); b) H. Yoshizawa, O. Ito and M. Matsuda, *Br. Poly. J.*, **20**, 441 (1988).
31) M. Arbelot, A. Samat, M. Rajzmann, M. Meyer, A. Gastaud, and M. Chanon, "Sulfur-Centered Reactive Intermediates in Chemistry and Biology," ed by C. Chatgilialoglu and K.-D. Asmus, Plenum Press, New York (1990), Ser. A: Life Sciences, Vol. 197, pp. 19—30.
32) E. Gentric, J. Lauransan, C. Roussel, and J. Metzger, *J. Chem. Soc., Perkin Trans. 2*, **1977**, 1015.
33) G. S. Hammond, *J. Am. Chem. Soc.*, **77**, 334 (1955).